Methodology for obtaining fractal parameters using petrophysical and pressure transient data for naturally fractured reservoirs

Lauro Jesús Vargas Muñoz
lauro.jesus.vargas@pemex.com
Pemex E&P/University of Calgary

Rodolfo Gabriel Camacho Velázquez
camachovrodolfo@gmail.com
Universidad Nacional Autónoma de México

Zhangxing (John) Chen
University of Calgary

María del Carmen Muñoz Ruiz
mrmcarmen@hotmail.com
Pemex E&P

Abstract

This work introduces a new methodology where the fractal parameters; fractal dimension (d_{mf}) and connectivity index (θ) can be computed by the analysis of petrophysical and pressure transient data. This methodology identifies, validates and analyzes naturally fractured reservoirs (NFR) with non-Euclidean geometry and no matrix participation; the fractal parameters (d_{mf} and θ) are calculated by the application of the derivative technique on well pressure transient response, and by the application of the rescaled range analysis based on well logs data. Additionally, the permeability and skin factor are computed based on the two equations proposed.

The practical application of this methodology is illustrated through the reliable results obtained from two field cases, where the fracture density (d_{mf}) and the connectivity of the fractures network (θ) were quantitative measured. This study shows that these fractal parameters play an important role on production performance.

Currently, the fractal parameters can be obtained by analyzing only pseudo stationary flow from pressure response, in field cases few well tests are run long enough in time to identify it. Likewise, the methodology introduced in this work allows to compute the fractal parameters by only analyzing the transient pressure response and petrophysical data, obtaining reliable estimations to support activities to reduce the uncertainty in the development of the field.

Keywords: Fractal parameters, petrophysical data, transient data, naturally fractured deposits.

Metodología para la obtención de parámetros fractales usando datos petrofísicos y datos de transientes de presión para yacimientos naturalmente fracturados

Resumen

Este trabajo introduce una nueva metodología donde los parámetros fractales; la dimensión fractal (d_{mf}) y el índice de conectividad (θ) se pueden calcular mediante el análisis de datos petrofísicos y de transientes de presión. Esta metodología identifica, valida y analiza YNF sin participación de matriz; los parámetros fractales (d_{mf} y θ) se calculan mediante la

aplicación de la técnica derivada en la respuesta de transiente de presión del pozo y por la aplicación del análisis de rango re-escalado basado en datos de registros de pozos.

La aplicación práctica de esta metodología se demuestra a través de los resultados obtenidos de un caso de campo en el que se midió cuantitativamente la densidad de fractura (d_{mf}) y la conectividad entre las fracturas (θ). Este estudio muestra que estos parámetros fractales desempeñan un papel importante en el comportamiento de la producción.

En la actualidad, los parámetros fractales pueden obtenerse analizando únicamente el flujo pseudo estacionario a partir de la respuesta de presión de fondo. En casos de campo, pocas pruebas de pozo son lo suficientemente largas como para identificar este periodo de flujo. Asimismo, la metodología introducida en este trabajo permite calcular los parámetros fractales analizando únicamente la respuesta del transiente de presión y datos petrofísicos, obteniendo resultados confiables para que puedan reducir la incertidumbre en el desarrollo de un campo.

Palabras clave: Parámetros fractales, datos petrofísicos, datos de transientes, yacimientos naturalmente fracturados.

Introduction

Chang and Yortsos (1990), Olarewaju (1996), Beier (1994) and Camacho (2001) have applied fractal models to pressure transient responses of naturally fractured reservoirs, where the main premise is that different scales, poor fracture connectivity and disorderly spatial distribution are present in the reservoir and a fractal fracture network is embedded in an Euclidean matrix, **Figure 1**. The Bourdet derivative technique is the best tool to identify fractal behavior, where the well bore pressure is a power law function of time and the spectral dimension can be calculated. This parameter is a function of two fractal parameters: fractal dimension (d_{mf}) and connectivity index (θ). The pressure transient responses of such models using the Bourdet derivative on a log log plot are two parallel straight lines, one for the pressure change and another for the pressure derivative, with the same slope; the slope value may be an indication of the fractal flow behavior.
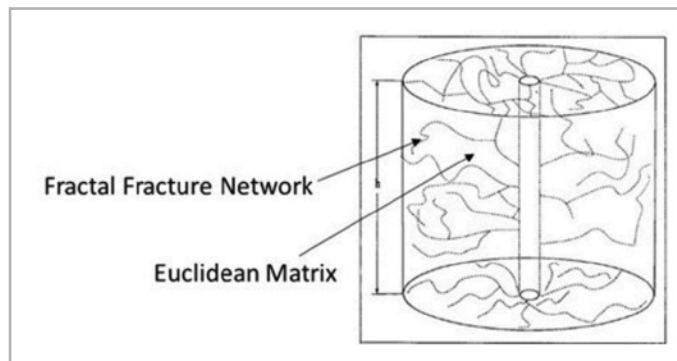
Figure 1. Fractal model description by Chang and Yortsos, (1990).

Fractals are geometric objects that remain statistically invariant upon a change of scale. A basic characteristic of fractal objects is that many of their properties, defined as volume averages over a region of scale (r), are scale dependent and statistically vary with a power law behavior. In **Figure 2** there are three fracture network examples, where the network 2a corresponds to a single fracture only, the mass of a fracture network (one fracture), with a d_{mf}=1 and d=2, where d_{mf} is the mass fractal dimension and d is the Euclidean dimension (embedding dimension), the network 2b due to its fractal structure, it has a power law behavior but now with a higher fracture density, $1<d_{mf}<2$, finally the network 2c which is the more traditional network, which has a constant fracture density with a d_{mf}=d=2. This network represents the typical Warren and Root double porosity model.
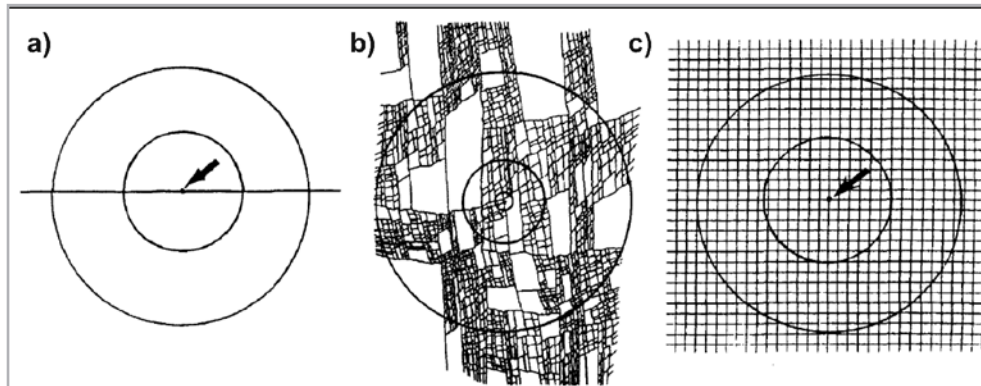
Figure 2. Networks in a 2D embedding medium d=2. a) d_{mf} =1 (Euclidean),b) 1< d_{mf} <2 (Fractal), and c) d_{mf} =2 (Euclidean) by Chang and Yortsos (1990).

1) Fractal parameters

The mass fractal dimension parameter (d_{mf}) gives information related to the fracture density in a porous medium; **Figure 3** shows three examples of 2D synthetic fractal networks with different fractal dimensions; as d_{mf} increases the fracture density increases and viceversa.
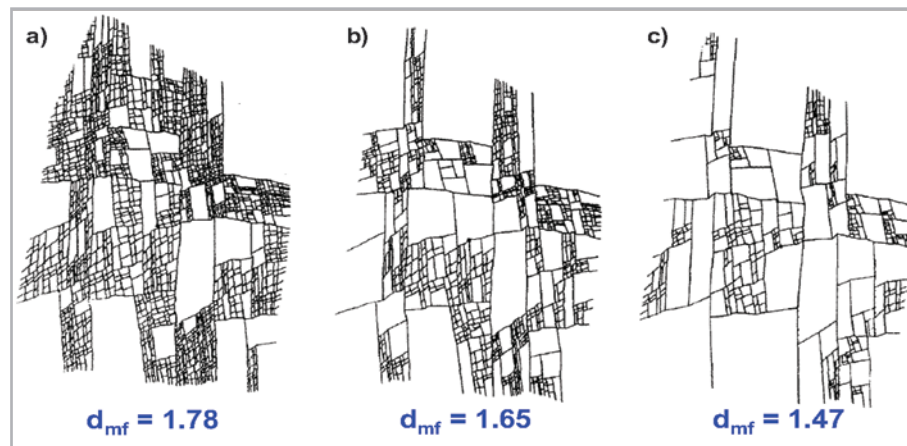
Figure 3. Fractal networks in 2D with different fractal dimensions by Acuña and Yortsos, (1995)[2].

The exponent θ (connectivity index) is related to diffusion or conduction. This parameter is related to the spectral exponent. The spectral dimension δ carries information about a mass fractal dimension and the connectivity index. This parameter is defined by applying the derivative technique; by analyzing the pressure transient flow response, the spectral dimension can be calculated. The parameter d_{mf} and θ cannot be calculated by the current methodologies by only analyzing the transient pressure responses, unless an optimization algorithm is used for this purpose or it is used

an approximate analysis like that shown by R. Posadas and R. Camacho (2016).

The spectral dimension defines the type of flow behavior based on:

a) If the value of the spectral dimension (δ) is < lower than 1, then the expected value of dmf is < lower than 2, it indicates that flow behavior is between linear and radial.

This expression suggests that the log log plots of pressure and derivative vs time will appear as two straight parallel lines. The pressure derivative vs time in a log-log plot will be a straight line, with a positive slope, **Figure 4**. The spectral dimension is calculated from the following equation.

$$\delta = 1 - m \qquad (1)$$
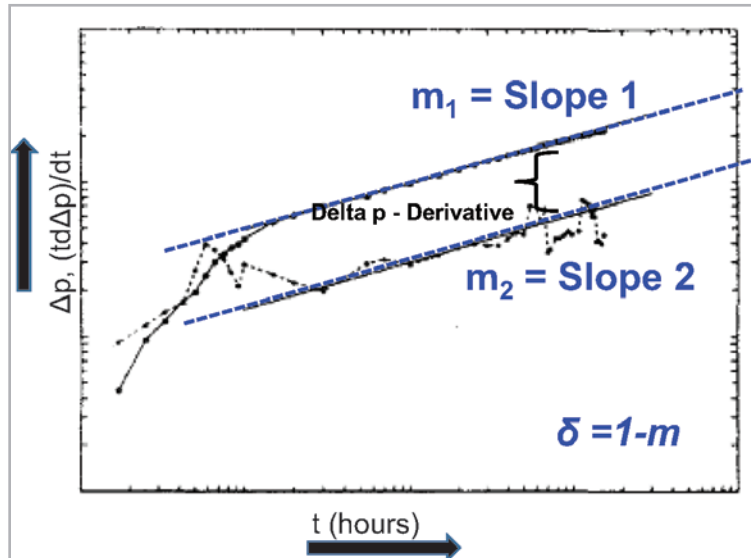
Figure 4. Log-log plot, typical fractal behavior when δ < 1.

2) Methodology proposed

2.1) Validation of a fractal behavior

In order to validate a fractal behavior, the semi-logarithmic derivative technique is applied. The following characteristics must be considered:

- Storage and production time effects before a buildup test, mainly because both tend to mask the reservoir behavior, i.e. power law behavior, (fractal geometry).

- The slopes measured from a buildup or drawdown test in a log-log (Log Δp, Log t Δp' vs Log time) have to be the same for both pressure and pressure derivative. This behavior must remain more than ½ cycle in the log-log plot in order to be significant.

- Compare the value obtained from the difference between pressure and the pressure derivative data at a defined time from a log log plot Figure 4 vs the difference calculated from the equation log (1/m), where m is the value of the slope; both values have to be similar.

2.2) Calculation of the spectral dimension (δ) from pressure transient test.

After of the validation of the fractal behavior, the spectral dimension can be calculated by the equation 1, if the value of δ is less than 1, then the expected value of dmf is going to be less than 2 indicating that flow behavior intermediate is between linear and radial, at this moment only the value of spectral dimension is calculated, **Figure 4**.

2.3) Calculation of the fractal dimension (d_{mf}) based on petrophysical data.

2.3.1) Introduction

A Rescaled range analysis (R/S) was invented by Hurst (1880-1978) by quantifying the long term discharge variations of the River Nile (1965), defining the Hurst exponent which is used as a measure of long term memory of time series in a fractal analysis. The Hurst exponent is denoted by (H), which is related to the fractal dimension. For a geological analysis where no theoretic fractal dimension is available, it is normally estimated from known samples by different approaches, such as a spectral density analysis and rescaled range (R/S). Hewett (1986) observed that the scaling relations of the spatial correlation in fractal distributions can be determined from the asymptotic behavior of the rescaled range (R/S), in conjunction with other tools of geostatistics [36].

Later, the method was proved resulting in an efficient technique for analyzing one dimensional fractal variables (Mandelbrot and Van Ness, 1968; Mandelbrot and Wallis, 1968, 1969).

Mandelbrot and Wallis (1969) and Feder (1988) established Equations 2, 3 and 4 to obtain the fractal dimension of a given sequence [16]. For a determined one-dimensional process, $Z(t)$ corresponds to the wire line log curve and the partial sample sequential range $R(t, n)$ of $Z(t)$.

$$R(t, n) = \max_{0<u<n}\left\{\sum_{i=1}^{u} Z(t+i) - \left(\frac{u}{n}\right)\sum_{j=1}^{n} Z(t+j)\right\} - \min_{0<u<n}\left\{\sum_{i=1}^{u} Z(t+i - \left(\frac{u}{n}\right)\sum_{j=1}^{n} Z(t+j)\right\} \qquad (2)$$

Where u is a discrete integer –value, a sample number corresponding to depth for wire line log readings (equivalent to time in a time series application); n is the time-span considered indicating the sequence interval or the number of data points ($n+1$) of the calculated range; and t is the start point (first sample number) of the samples used for calculation. The ranges of different processes, $R(t, n)$ must be compared; the sample variance S^2 is defined in Equation 3 [24].

$$S^2 = 1/n \sum_{i=1}^{n} Z^2(t+i) - \left[\frac{1}{n}\sum_{j=1}^{n} z(t+j)\right]^2 \qquad (3)$$

A process is considered to be fractal when the log-log plot of R/S versus the number of ranges shows an aligned straight line. The slope of this line is called the Hurst exponent (H), **Figure 5**, which is related to the local fractal dimension d_{mf}, Equation 4.

$$d_{mf} = 2 - H . \qquad (4)$$
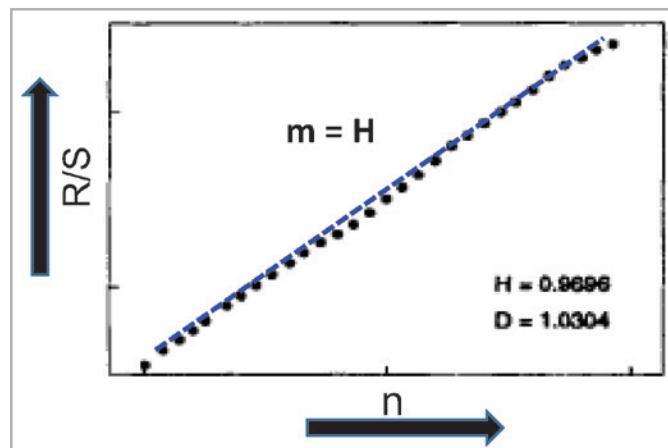
Figure 5. Example of R/S analysis, log-log plot.

2.3.2) Methodology to calculate the fractal dimension, (dmf).

2.3.2.1) Considerations

Data from wire line logs must correspond to reservoir section. The logs more suitable for this analysis can be sonic, gamma ray and neutron logs, because they give us information about lithology. If the reservoir has several formations, it is important to do the analysis for each formation separately.

According to Mandelbrot and Wallis (1969) and Feder (1988), the sample set must be greater than 1000 points in order to get a reliable Hurst exponent (*H<1*) and get a reliable analysis. On the other hand if *H* is greater than 1, it means that there are not enough data sets, resulting in an unreliable value of *H* [24,36].

2.3.2.2) Methodology

The following proposed methodology explains step by step how to obtain the fractal dimension from the Hurst exponent.

a) Estimation of H:

1. Select the petrophysical data to analyze from well logs responses.

2. Define the range of data sets because the rescaled range is based on multiple ranges of data.

3. Calculate the mean for each range and for the total data.

$$\textbf{mean}_s = \textbf{m}_s = \frac{1}{n}\sum_{i=1}^{n}\textbf{X}_i \qquad (5)$$

where:

s = series of data
n = the size of the range for which the mean is calculated
X = the value of one element in the range selected

4. Create a series of deviations for each range. This creates another series of data using the mean of each range.

$$\boldsymbol{Y_t = X_t - m; for\ t = 1, 2.., n} \dots \qquad (6)$$

where:

Y = the new time series adjusted for deviations from the mean
X = the value of one element in the range selected
m = the mean for the range calculated previously

5. Create a series, considering the total of deviations from the mean in order to get a series of deviations from the mean for each range.

$$y = \sum_{i=1}^{t} Y_t \qquad (7)$$

where:

y = total of the deviations from the mean for each series
Y = the series adjusted for deviations from the mean

6. Calculate the widest difference in the series of deviations. Find both the maximum and minimum values in the series of deviations for each range. Take the difference between the maximum and minimum in order to calculate the widest difference.

$$R_t = \max(Y_1, Y_2, \ldots, Y_t; -\min(Y_1, Y_2, \ldots, Y_t) \text{ for } t = 1,2, \ldots, n \qquad (8)$$

where:

R = the widest spread in each range
Y = the value of one element in the "deviations from the mean" range

7. Calculate the standard deviation (S) for each range. There will be a standard deviation calculation for each range and for the total set of data.

$$\sigma = \sqrt{\frac{1}{t}\sum_{i=1}^{t}(X_i - m)}^{\ 2} \qquad \text{for } t=1, 2 \ldots n \qquad (9)$$

8. Calculate the rescaled range (R/S) for each one. This step creates a new measure for each range in the time series that shows how wide the range is measured in standard deviations by dividing the value obtained in step 6 (R) by the standard deviation for each range (S) in step 7.

9. Build a table with the numbers of ranges defined and the values of R/S calculated for each range.

10. Plot the R/S vs n (number or ranges) in a log-log plot. The slope calculated from this plot is the Hurst exponent.

11. The mass fractal dimension (d_{mf}) is calculated by Equation 4.

2.3.3) Methodology to calculate the connectivity index (θ).

The exponent θ (connectivity index) which is related to the connectivity between fractures; if θ= 0 it means that all the fracture network is connected (Euclidean case), if θ >0 it means that the connectivity among fractures is decreasing, (fractal case), until it reaches a value of 1, which means a disconnected fracture network.

Finally the fractal parameter θ can be calculated by the following equation:

$$\delta = (d_{mf}) / (2+\theta). \tag{10}$$

where:

δ is the spectral dimension, (obtained from pressure transient test)
d_{mf} is the fractal dimension, (obtained from statistical analysis based on petrophysical data)

2.3.4) Calculation of permeability (kw) and skin factor (s) for fractal reservoirs

The calculations of the permeability (k_w) and the skin factor (s) are very important because they indicate if a reservoir requires activities such as: minor or major workovers, stimulations, and fracturing, in order to increase the oil and gas production of the oilfield. To compute the permeability and skin factor for fractal reservoirs, the fractal parameters such as fractal dimension (d_{mf}) and connectivity index (θ) must have to be considered. This is the reason for developing a methodology to compute them. The two equations proposed were based on the equation 11 from the paper SPE 71591[21], for an infinite fractal reservoir without matrix fracture transfer.

$$p_{wD}\,(t_D) = \frac{1}{-v\,(2+\theta)} + \frac{(2+\theta)^{2v-1}}{v\Gamma\,(1-v)}\, t_D^v \tag{11}$$

For this analysis the variable skin factor (s) was added, modifying the original equation 11, obtaining the following equation:

$$p_{wD}\,(t_D) = \frac{1}{-v\,(2+\theta)} + \frac{(2+\theta)^{2v-1}}{v\Gamma\,(1-v)}\, t_D^v + s \tag{12}$$

Equation 12 is given in dimensionless variables and the behavior of this equation depends on whether $v > 0$ or $v < 0$, where v is given by Equation 15. The first case considers $d_{mf} < 2$, resulting in a log-log plot of pressure and pressure derivative versus time in two parallel straight lines with positive slope.

where:

$$t_D = \frac{0.0002637 k_w(t)}{\phi_w \mu r_w^\theta C_t} \tag{13}$$

$$p_D = \frac{k_w(h)(\Delta p)}{141.2\ q\mu B} \tag{14}$$

$$v = \frac{1-\text{ß}}{\theta+2} \tag{15}$$

$$\text{ß} = d_{mf} - \theta - 1 \tag{16}$$

d_{mf}: Fractal dimension

θ: connectivity index

Γ: gamma function

s: skin factor

k_w: permeability (md)

t: time (hours)

Δ_p: pressure drop (psi)

φ_w: Porosity (fraction), from core analysis

μ: viscosity (cp)

r_w: well radius (ft)

c_i: Total compressibility (psi^{-1})

B: oil formation factor (RB/STB)

q: oil flow rate (STB/D)

h: formation thickness (ft)

Substituting Equations 13 and 14 in Equation 12, Equation 17 was obtained:

$$\frac{k_w h \Delta p}{141.2 q \mu B} = \frac{1}{-v(2+\theta)} + \frac{(2+\theta)^{2v-1}}{v\Gamma(1-v)}\left(\frac{0.0002637 k_w(t)}{\phi_w \mu r w^\theta\, Ct}\right)^v + s \tag{17}$$

From Equation 17; Δp for fractal reservoirs was defined by the following equation:

$$\Delta p = \frac{141.2 q \mu B}{k_w h}\left(\frac{1}{-v(2+\theta)}\right) + \frac{q \mu B}{k_w h}\left(\frac{(2+\theta)^{2v-1}}{v\Gamma(1-v)}\right)\left(\frac{k_w}{\phi_w \mu r w^\theta\, Ct}\right)^v t^v + \frac{141.2\, q \mu B}{k_w h}\, s \tag{18}$$

From Equation 18, the slope is defined by the following equations.

$$m = \frac{141.2 q \mu B}{k_w h}\left(\frac{(2+\theta)^{2v-1}}{v\Gamma(1-v)}\right)\left(\frac{0.0002637 k_w}{\phi_w \mu r w^{2+\theta}\, Ct}\right)^v \tag{19}$$

$$m = \frac{141.2 q \mu B}{h}\left(\frac{(2+\theta)^{2v-1}}{v\Gamma(1-v)}\right)\frac{0.0002637 k_w^v}{k_w}\frac{1}{(\phi_w \mu r w^{2+\theta}\, Ct)^v} \tag{20}$$

$$m = \frac{141.2 q \mu B}{h}\left(\frac{(2+\theta)^{2v-1}}{v\Gamma(1-v)}\right)\left(\frac{1}{(\phi_w \mu r w^{2+\theta}\, Ct)^v}\right)0.0002637 k_w^{v-1} \tag{21}$$

Finally from Equation 21, the proposed equation to compute k_w was defined:

$$k_w^{v-1} = \frac{m}{\frac{q \mu B}{h}\left(\frac{(2+\theta)^{2v-1}}{v\Gamma(1-v)}\right)\left(\frac{1}{(\phi_w \mu r w^{2+\theta}\, Ct)\ v}\right)} \tag{22}$$

From Equation 22 the permeability can be obtained; however, in order to apply it, the slope (*m*) must be known. For this the following procedure was proposed:

- From buildup test data calculate Δ_p (psi)

- From Equation 15,ν is calculated

- From buildup test data calculate the $time^\nu$;

- Build a Cartesian plot *(Δp vs $time^\nu$)* from the buildup test,

- The straight line identified in the Cartesian plot is the slope (*m*) in $\frac{psi}{hour^\nu}$.

In order to compute the skin factor, Equation 18 was considered, leading to Equation 4-18.

$$\Delta p = (m)\,(t) + \frac{q\mu B}{k_w h}\left(\frac{1}{-v(2+\theta)}\right) + \frac{q\mu B}{k_w h}s \tag{23}$$

Then intercept (b) was defined by the following equation:

$$b = \frac{q\mu B}{kwh}\left(\frac{1}{-v(2+\theta)} + s\right) \tag{24}$$

Where *b=Δp (psi);* **Figure 6**

Finally, from Equation 24, the following equation was defined:

$$S = \frac{bhk_w}{141.2\ q\mu B} - \left(\frac{1}{-v(2+\theta)}\right) \tag{25}$$

3) Validation of methodology, (field cases)

The idea of this research started in 2013, when two buildup tests from NFRs of the southwest of Mexico, showed a possible fractal behavior in a log log plot of pressure and pressure derivative versus time. The necessity to establish a methodology in order to analyze this type of behavior was identified. These two cases were analyzed using the methodology explained previously: first, the validation of a fractal behavior; second, obtaining the fractal parameters; finally, identifying how these parameters influence the rate flow production of the field.
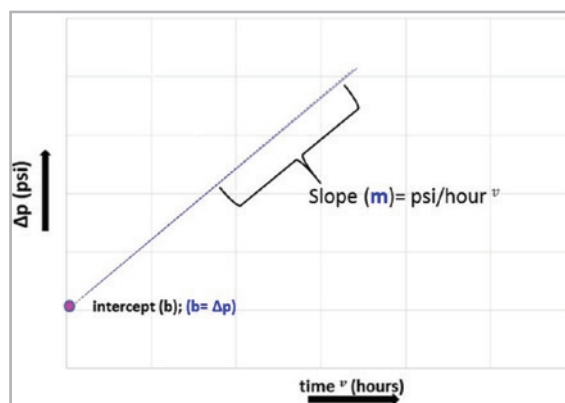
Figure 6. Δ_p vs $time^\nu$, Cartesian plot.

3.1) Field case, (reservoir S)

A combined analysis of well testing and production data for a well producing in a field located in the southwest region of Mexico is presented in this section to explain the methodology proposed.

"S" is a black oil reservoir, at an average depth of 3,600 meters, complex NFR. The formation was deposited during the Upper Cretaceous. Detailed geological data has defined an average porosity of 9%. Recent well tests and well-logging studies have estimated an average permeability value of 9 md, for those wells which have Euclidean geometry. The reservoir S has nine oil producer wells, 3 wells produced from the formation Maastrichtian Upper Cretaceous, and 6 wells produced from the Maastrichtian Upper Cretaceous, **Figure 7**. The matrix in this field is compact, and does not participate in the hydrocarbon production, and therefore, a single porosity analysis was applied. The analysis of this research is based on the wells from the Campaniano Upper Cretaceous, only one well (S-316) showed fractal behavior and the other 5 wells showed Euclidean geometry.
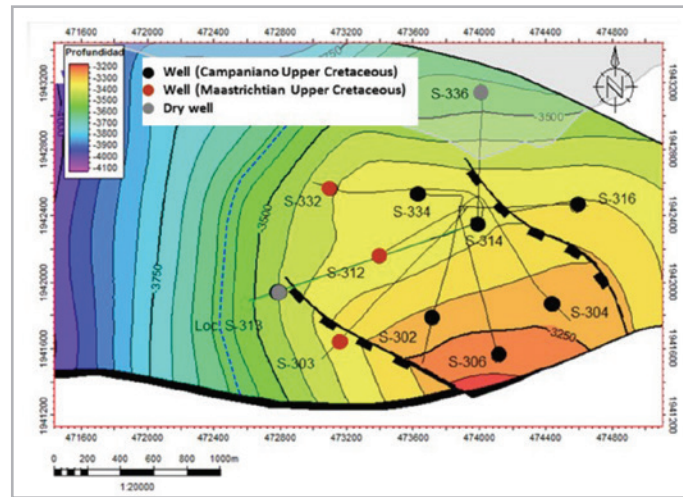
Figure 7. Reservoir S, (contour map from the formation Upper Cretaceous).

Only four wells have buildup tests (S-302, S-304, S-314, and S-316). Three of these tests were analyzed using the semi logarithmic derivative technique, see **Figure 8**. The results obtained from the wells with Euclidean geometry are shown in **Table 1**.
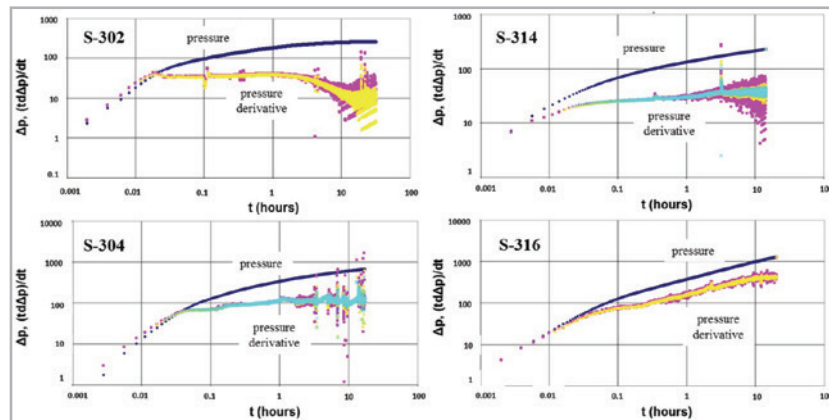
Figure 8. Log log plots of pressure and pressure derivative versus time. (Well from Field S- Campaniano Upper Cretaceous).

Table 1. Well tests analysis results from wells with Euclidean geometry.

Well	K (md)	kh (md/ft)	s (skin factor)	Model
S-302	17.6	4044	-3.7	
S-304	4.6	921	0.05	Radial homogeneous
S-314	19.8	9422	-1.6	

Well S-316

Validation of fractal behavior:

According to the proposed methodology, the first step was to identify the fractal behavior. **Table 2** shows the input data for well S-316.

Table 2. Input data, well S-316.

Well	S-316	
h	650	ft
Ct	4.5 exp-5	PSI -1
Oil rate	856	stb/d
rw	0.27	ft
API	30	
μ	0.8	cp
Bo	1.6	m3/m3
Production time before build up test	320	hours

The semi logarithmic derivative technique was applied in order to identify the fractal behavior, **Figure 9**. First, it is important to identify the period of time in the buildup test without production effects. For this well the production time before the buildup test was 320 hours. This means that only the first 32 hours from the buildup test are a reliable reservoir response, without production time effects. Second, the validation of the fractal behavior is based on the slopes measured in the log log plot of pressure and pressure derivative versus time, Figure 9. Both of these slopes must be the same. This behavior must remain for more than at least ½ cycle in the log log plot. Third, we compare the difference between pressure and pressure derivative at defined times from the log–log plot vs the value calculated from the equation: (*1/m*). Both of these must be similar, **Table 3**.
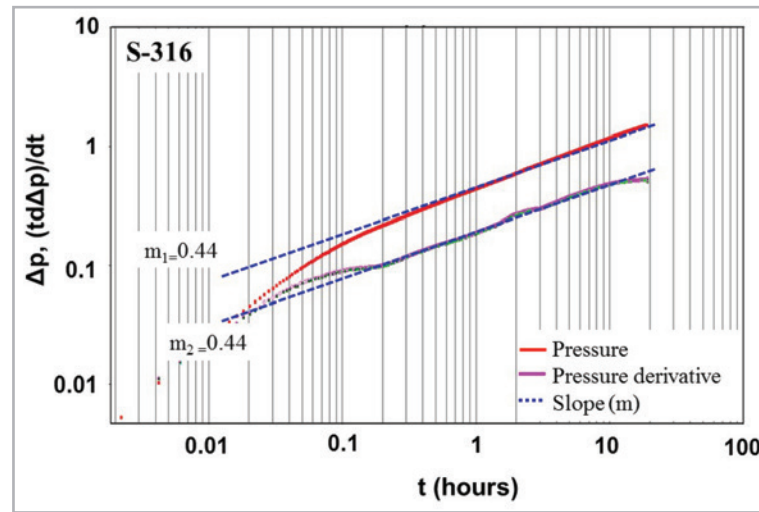
Figure 9. Log log plot of pressure and pressure derivative versus time, (Well S-316).

Table 3. Results (validation of fractal behavior).

m1	0.46
m2	0.46
Log (1/m)	0.34
pressure - pressure derivative @ 1 hour	0.33
Conclusion	Fractal geometry

Determination of fractal parameters:

Once the fractal behavior was validated, the second step was to calculate the fractal parameters: spectral dimension (δ), fractal dimension (d_{mf}) and the connectivity index (θ). First, from the well pressure transient response the spectral dimension was calculated, obtaining the following results, **Table 4**.

Table 4. Results from pressure transient response.

δ (spectral dimension)	0.54
Case $\delta < 1$:	$d_{mf} < 2$ (flow behavior intermediate between linear and radial).

Table 4. Ranges for R/S analysis.

R/S	(number of range)
12.8	1
45	2
92.7	3
92.5	4
130.7	5

According to the spectral dimension value, the expected fractal dimension for this case must be less than 2 and the flow regime present in the reservoir is between linear and radial flow. Then according to the methodology proposed in this research, the next step is to apply the rescaled range analysis based on wireline log responses, in order to calculate the fractal dimension, and consequently the connectivity index.

Rescaled range analysis:

First, this analysis was based on the sonic well log responses from the Upper Cretaceous formation, and approximately 1,100 data points were considered. The data was divided in 5 ranges, Table 4, where the statistical analysis was applied (mean and standard deviation) in order to obtain the relationship, (R/S).

Second, based on the information showed in Table 4 the calculation of the Hurst exponent was based on a log log plot (R/S vs n). The slope defined was based on the data related to the reservoir zone; in this case Upper Cretaceous formation. The slope is called the Hurst exponent, **Figure 10**. Third, the fractal dimension and connectivity index (θ) were computed based on the methodology proposed; see **Table 5** for results. In conclusion, the assumption defined by the calculation of the spectral dimension (δ) from pressure transient response, where d_{mf} is less than 2, was validated. As mentioned before, d_{mf} indicates the fracture density present in the reservoir. To understand the value of d_{mf} =1.14, the fractal network in 2D proposed by Acuna and Yortsos (1995) was used. The lowest value of d_{mf} was 1.47. Therefore, the fracture density is poor, lower than the worst case presented by Acuna and Yortsos, (Figure 3). According to the value calculated of d_{mf} for well S-316, the fracture density is really low. Second, the connectivity index is slightly greater than 0 (θ=0.11), which indicates that the fractures are reasonably well connected. Finally, the next step is to evaluate the effect of these parameters on production decline.
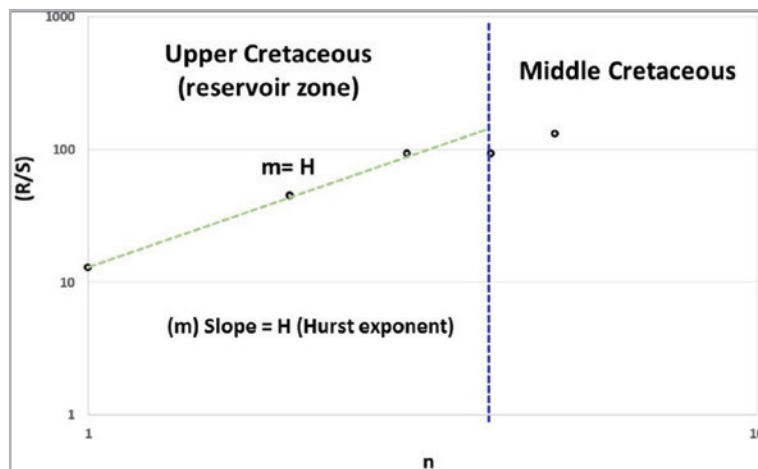
Figure 10. Log log plot; R/S versus the number of ranges, (Well S-316).

Table 5. Results.

Hurst exponent (H)	0.86
d_{mf}	1.14
θ	0.11

Effect of fractal parameters on production decline

In order to evaluate the effects of fractal parameters on oil rate behavior in well S-316, it was necessary to compare the oil rate from Euclidean geometry wells vs well S-316 with fractal geometry from Campaniano Upper Cretaceous formation, based on a normalized semilog plot ($q\ /\Delta p\ (BPD/$ PSI) vs *time* (hours), **Figure 11**. As expected, the flow rate from the fractal case (well S-316) is smaller than in the Euclidean cases (Wells 334,306,304,314 and 302), in which the diffusion is faster because the fracture density is uniform and all the fractures are connected. On the other hand in the fractal case the oil is produced from finite connected clusters only in a poor fracture density medium.
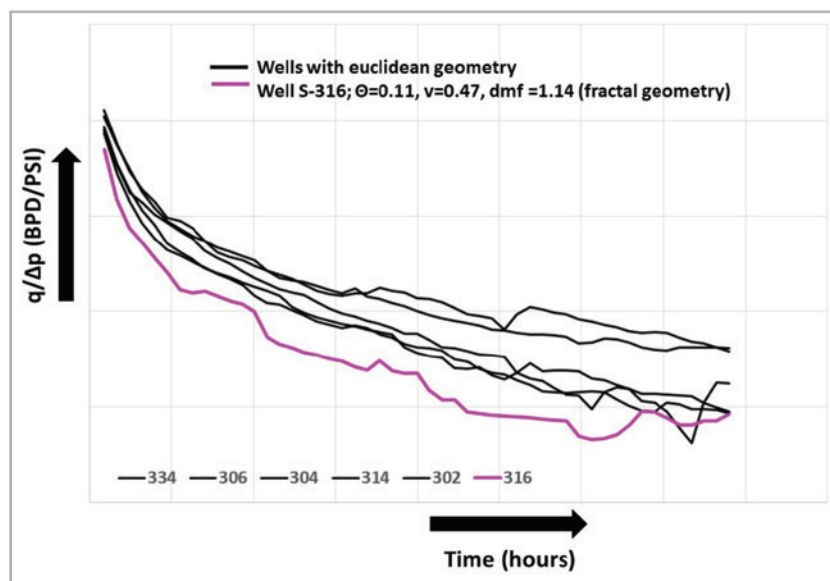
Figure 11. Normalized semi log plot ($q/\Delta p$ (BPD/PSI) vs time, (hours).

Conclusions

This study contains details of analyzing NFR with fractal geometry and without matrix participation. Two field cases were analyzed with the methodology proposed. The study leads to the following conclusions and recommendations:

- Methodology to identify and analyze NFR with fractal geometry with no matrix participation was defined and equations to compute kw and s for NFR with fractal geometry were obtained.

- For these types of reservoirs the fracture density and connectivity between fractures play an important role in production performance.

- If these reservoirs are still treating as reservoirs with Euclidean geometry; a wrong understanding

of the fracture density and their connectivity would be obtained, resulting in: unproductive wells, very optimistic production forecast, inefficient primary, secondary and enhanced oil recovery methods.

- It is recommended to apply the same methodology in NFR with matrix participation and then evaluate the effects of matrix – fracture coefficients and fractal parameters on the production performance.

- It is also highly recommended to consider the fractal parameters in reservoir simulation models in order to compute realistic production forecasts, and then establish the best strategy to increase the oil and gas recovery factors.

References

1. Acuna J. A. and Yortsos Y. C. 1991. Numerical Construction and Flow simulation in Network of fractures using Fractal Geometry. Presented at the SPE Annual Technical Conference and Exhibition, Dallas, Texas, USA, 6-9 October. SPE-22703-MS. https://doi.org/10.2118/22703-MS.

2. Acuna, J. A., Ershaghi, I., and Yortsos, Y. C. 1995. Practical Application of Fractal Pressure Transient Analysis of Naturally Fractured Reservoirs. *SPE Form Eval* **10** (3): 173-179. SPE-24705.PA. https://doi.org/10.2118/24705-PA.

3. Albinali, A., Holy, R., Sarak, H. et al. 2016. Modeling of 1D Anomalous Diffusion in Fractured Nanoporous Media. *Oil & Gas Science and Technology – Rev. IFP Energies Nouvelles* **71** (4). https://doi.org/10.2516/ogst/2016008.

4. Aguilera, R. 1987. Well Test Analysis of Naturally Fractured Reservoirs. *SPE Form Eval* **2** (3): 239-252. SPE-13663-PA. https://doi.org/10.2118/13663-PA.

5. Aguilera, R. 1995. *Naturally Fractures Reservoirs*, second edition. Tulsa Oklahoma: PennWell Publishing Company.

6. Aguilera, R. 2003. Integration of Geology Petrophysics and Reservoir Engineering for Characterization of Carbonate Reservoirs Through Pickett Plots. *AAPG Bulletin* **88** (4): 433-446. https://doi.org/10.1306/12010303071.

7. Barenblantt, G. I. and Zheltov, I. P. 1960. Fundamentals Equations of Filtration of Homogeneous Liquids in Fissured Rocks. *Soviet Dokl. Akd. Nauk.* **13** (2): 545-548.

8. Barton C. C., Scholz C. H., Schutter T. et al. 1991. Fractal Nature of Hydrocarbon Deposits—2: Spatial Distribution. AAPG Annual Convention, Dallas, Texas, USA, 7-10 April. Article #91004.

9. Beier, R. A. 1990. Pressure Transient Field Data Showing Fractal Reservoir Structure. Presented at the CIM/SPE International Tech. Meeting, Calgary, Alberta, Canada, 10-13 June. SPE-21553-MS. https://doi.org/10.2118/21553-MS.

10. Beier, R. A. 1994. Pressure-Transient Model for a Vertically Fractured Well in a Fractal Reservoir. *SPE Form Eval* **9** (2): 122-128. SPE-20582-PA. https://doi.org/10.2118/20582-PA.

11. Camacho- Velázquez, R. G., Vásquez-Cruz, M., Castrejón-Aivar, R. et al. 2005. Pressure-Transient and Decline-Curve Behavior in Naturally Fractured Vuggy Carbonate Reservoirs. *SPE Res Eval & Eng* **8** (2): 95-112. SPE-77689-PA. https://doi.org/10.2118/77689-PA.

12. Camacho-Velázquez, R. G., Fuentes-Cruz, G., and Vásquez-Cruz, M. 2008. Decline Curve Analysis of Fractured Reservoirs with Fractal Geometry. *SPE Res Eval & Eng* **11** (3): 606-619. SPE-104009-PA. https://doi.org/10.2118/104009-PA.

13. Capuano, R. M. 1993. Evidence of Fluid Flow in Micro Fractures in Geopressured Shale. *AAPG Bulletin* **77** (8): 1303-1314.

14. Chang, J. and Yortsos, Y. C. 1990. Pressure transient Analysis of Fractal Reservoirs. *SPE Form Eval* **5** (1): 31-38. SPE-18170-PA. https://doi.org/10.2118/18170-PA.

15. Coalson, E. B., Hartmann, D. J., and Thomas, J. B. 1985. Productive Characteristics of Common Reservoir Porosity Types. *Bulletin of the South Texas Geological Society 15* (6): 35-51.

16. Coconi-Morales, E., Ronquillo-Jarillo, G., and Campos-Enríquez, J. O. 2010. Multi-scale Analysis of Well-logging Data in Petrophysical and Stratigraphic Correlation. *Geofísica Internacional 49* (2), 55-67.

17. Crane, S. E. and Tubman, K. M. 1990. Reservoir Variability and Modeling With Fractals. Presented at the SPE Annual Technical Conference and Exhibition, New Orleans, Louisiana, USA, 23-26 September. SPE-20606-MS. https://doi.org/10.2118/20606-MS

18. De Swaan-O., A. 1976. Analytical Solutions for determining Naturally Fractured Reservoirs Properties by Well Testing. *SPE J. 16* (3): 117-122. SPE-5346-PA. https://doi.org/10.2118/5346-PA.

19. De Swaan-O., A., Camacho-Velázquez, R. G., and Vásquez-Cruz, M. 2012. Interference Tests Analysis in Fractured Formations with a Time-Fractional Equation. Presented at the SPE Latin American and Caribbean Petroleum Engineering Conference, Mexico City, Mexico, 16-18 April. SPE-153615-MS. https://doi.org/10.2118/153615-MS.

20. Ershaghi, I. and Rhee, S.-W. 1976. Analysis of Pressure Transient Data in Naturally Fractured Reservoirs with Spherical Flow. Presented at the SPE Annual Fall Technical Conference and Exhibition, New Orleans, Louisiana, USA, 3-6 October. SPE-6018-MS. https://doi.org/10.2118/6018-MS.

21. Feder, J. 1988. *Fractals*. New York: Plenum Press.

22. Flamenco-López, F. and Camacho-Velázquez, R. G. 2001. Fractal Transient Pressure Behavior of Naturally Fractured Reservoirs. Presented at the SPE Annual Fall Technical Conference and Exhibition, New Orleans, Louisiana, USA, 30 September-3 October. SPE-71591-MS. https://doi.org/10.2118/71591-MS.

23. Flamenco-López, F. and Camacho-Velázquez, R. G. 2003. Determination of Fractal Parameters of Fractured Networks Using Pressure-Transient Data. *SPE Res Eval & Eng 6* (1): 39-47. SPE-82607-PA. https://doi.org/10.2118/82607-PA.

24. Friedman, M. and McKiernan, D. E. 1995. Extrapolation of Fracture Data from Outcrops of The Austin Chalk in Texas to Corresponding Petroleum Reservoirs at Depth. *J Can Pet Technol 34* (8). PETSOC-95-08-04. https://doi.org/10.2118/95-08-04.

25. Halbouty, M. T., ed. 2003. Giant Oil and Gas Fields of the Decade 1990-1999. Tulsa, Oklahoma: American Association of Petroleum Geology, Memoir 78.

26. Hardy, H. H. and Beier, R. A. 1994. *Fractals in Reservoir Engineering*. Singapore: World Scientific Publishing Co.

27. Hewett, T. A. 1986. Fractal Distributions of Reservoirs Heterogeneity and their Influence on Fluid Transport. Presented at the SPE Annual Fall Technical Conference and Exhibition, New Orleans, Louisiana, USA, 5-8 October. SPE-15386-MS. https://doi.org/10.2118/15386-MS.

28. Hubbert, M. K. and Willis, D. G. 1957. Mechanics of Hydraulic Fracturing. *Petroleum Trans.*, AIME **210**: 153-168. SPE-686-G.

29. Hurst, H. E., Black, R. P., and Simaika, Y. M. 1965. *Long-Term Storage: An Experimental Study*. London: Constable.

30. Jelmert, T. A. 2009. Productivity of Fractal Reservoirs. Presented at the SPE Saudi Arabia Section Technical Symposium, Al-Khobar, Saudi Arabia, 9-11 May. SPE-126080-MS. https://doi.org/10.2118/126080-MS.

31. Kong, X., Li, D., and Lu, D. 2009. Transient Pressure Analysis in Porous and Fractured Fractal Reservoirs. *Science in China Series E: Technological Sciences* 52: 2700. https://doi.org/10.1007/s11431-008-0245-z.

32. Kuykendall, M. D. and Fritz, R. D. 2001. Misener Sandstone of Oklahoma. American Association of Petroleum Geologists Search and Discovery Article No. 10018.

33. Li, K. and Zhao, H. 2011. Fractal Prediction Model of Spontaneous Imbibition Rate. *Transport in Porous*

Media **91** (2): 363-376. https://doi.org/10.1007/s11242-011-9848-0.

34. Lynch, M.T. 1990. *Evidence of Paleokarstification and Burial Diagenesis in the Arbuckle Group of Oklahoma*. MS Thesis, Oklahoma State University, Faculty of the Graduate College, Stillwater, Oklahoma.

35. Mandelbrot, B. B. and Wallis, J. R. 1969a. Computer Experiments with Fractional Gaussian Noises. Part 1: Average and Variances. *Water Resources Research* **5** (1): 228-241. https://doi.org/10.1029/WR005i001p00228.

36. Mandelbrot, B. B. and Wallis, J. R. 1969b. Computer Experiments with Fractional Gaussian Noises. Part 2: Rescaled Ranges and Spectra. *Water Resources Research* **5** (1): 2242-259. https://doi.org/10.1029/WR005i001p00242.

37. Mandelbrot, B. B. and Wallis, J. R. 1969c. Computer Experiments with Fractional Gaussian Noises. Part 3: Mathematical Appendix. *Water Resources Research* **5** (1): 260-267. https://doi.org/10.1029/WR005i001p00260.

38. Mandelbrot, B. B. 1983. *The Fractal Geometry of Nature*. New York: W. H. Freeman and Company.

39. Martin, A. J., Solomon, S. T., and Hartmann, D. 1997. Characterization of Petrophysical Flow Units in Carbonate Reservoirs. *AAPG Bulletin* **81** (7): 734-759.

40. Mathews, J. L., Emanuel, A. S., and Edwards, K. A. 1989. Fractal Methods Improve Mitsue Miscible Predictions. *J Pet Technol* **41** (11): 1136-1142. SPE-18327-PA. https://doi.org/10.2118/18327-PA.

41. McNaughton, D. A. 1953. Dilatancy in Migration and Accumulation of Oil in Metamorphic Rocks. *AAPG Bulletin* **37** (2): 217-231.

42. McNaughton, D. A. and Garb, F. A. 1975. Finding and Evaluating Petroleum Accumulations in Fractured Reservoir Rock. In *Exploration and Economics of the Petroleum Industry*, Vol.13, 23-49. New York: Matthew Bender & Company Inc.

43. Mead, W. J. 1925. The Geologic Role of Dilatancy. *Journal of Geology* **33** (7): 685-698.

44. Najurieta, H. L. 1980. A Theory for Pressure Transient Analysis in Naturally Fractured Reservoirs. *J Pet Technol* **32** (7): 1241-1250. SPE-6017-PA. https://doi.org/10.2118/6017-PA.

45. Nelson, R. A. 1975. *Fracture Permeability in Porous Reservoirs, an Experimental and Field Approach*. Ph.D. Dissertation, Texas A&M University.

46. Nelson, R. A. 1985. *Geologic Analysis of Naturally Fractured Reservoirs*. Houston, Texas: Gulf Publishing Company.

47. Olarewaju, J. S. 1996. Modeling Fractured Reservoirs with Stochastic Fractals. Presented at the Abu Dhabi International Petroleum Exhibition and Conference, Abu Dhabi, United Arab Emirates, 13-16 October. SPE-36207-MS. https://doi.org/10.2118/36207-MS.

48. Pang, J. and North, C. P. 1996. Fractals and their Applicability in Geological Wireline Log Analysis. *Journal of Petroleum Geology* **19** (3): 339-350. https://doi.org/10.1111/j.1747-5457.1996.tb00438.x.

49. Poon, D. 1995. Transient Pressure Analysis of Fractal Reservoirs. Presented at the Annual Technical Meeting, Calgary, Alberta, June 7- 9. PETSOC-95-34. https://doi.org/10.2118/95-34.

50. Posadas-Mondragón, R. and Camacho-Velázquez, R. G. 2016. Influence and Determination of Mechanical Skin in a Reservoir with a Fractal Behavior. Presented at the SPE Latin America and Caribbean Heavy and Extra Heavy Oil Conference, Lima, Peru, 19-20 October. SPE-181190-MS. https://doi.org/10.2118/181190-MS.

51. Raghavan, R. 2009. A Note on the Drawdown, Diffusive Behavior of Fractured Rocks. *Water Resources Research* **45** (2). W02502. https://doi.org/10.1029/2008WR007158.

52. Razminia, K., Razminia, A., and Torres, D. F. M. 2015. Pressure Responses of a Vertically Hydraulic Fractured

Well in a Reservoir with Fractal Structure. *Applied Mathematics and Computation* **257** (April): 374-380. https://doi.org/10.1016/j.amc.2014.12.124.

53. Restrepo Restrepo, D. P. 2000. *Análisis de Registros Verticales de Porosidad y su Aplicación al Modelamiento Fractal de un Yacimiento*. Tesis de Maestría, Universidad Nacional de Colombia, Posgrado de Recursos Hidráulicos.

54. Sahimi, M. and Yortsos, Y. C. 1990. Applications of Fractal Geometry to Porous Media: A Review. Society of Petroleum Engineering. SPE- 20476-MS.

55. Serra, K. V., Reynolds, A. C., and Raghavan, R. 1983. New Pressure Transient Analysis Methods for Naturally Fractured Reservoirs. *J Pet Tech* **35** (12): 2271-2283. SPE-10780-PA. https://doi.org/10.2118/10780-PA.

56. Shen, P., Liu, M. and Jia, F. 1998. Application of Fractal Techniques in Reservoir Development. Presented at the SPE International Oil and Gas Conference and Exhibition in China, Beijing, China, 2-6 November. SPE-50878-MS. https://doi.org/10.2118/50878-MS.

57. Stearns, D. W. and M. Friedman. 1972. Reservoirs in Fractured Rock: Geologic Exploration Methods. In *Stratigraphic Oil and Gas Fields: Classification, Exploration Methods, and Case Histories*, ed. R. E. King, 82-106. Tulsa, Oklahoma: American Association of Petroleum Geology, Memoir 16.

58. Stearns, D. W. 1982-1994. AAPG Fractured Reservoirs School Notes. Great Falls, Montana.

59. Warren, J. E. and Root, P. J. 1963. The Behavior of Naturally Fractured Reservoirs. *SPE J.* **3** (3): 245–255. SPE-426-PA. https://doi.org/10.2118/426-PA.

60. Zhao, Y. and Zhang, L. Solutions and Type Curve Analysis of Fluid Flow Model for Fractal Reservoir. *World Journal of Mechanics* **1** (5): 209-216. https://doi.org/10.4236/wjm.2011.15027.

Semblanza de los autores

Lauro Jesús Vargas Muñoz

Ingeniero petrolero egresado de la ESIA Unidad Ticomán del Instituto Politécnico Nacional. Maestro en ciencias por la University of Calgary.

Actualmente labora como Ingeniero de yacimientos, en la Subdirección de Aseguramiento Tecnológico, en Pemex Exploración y producción.

Rodolfo Gabriel Camacho Velázquez

Ingeniero geofísico egresado de la Universidad Nacional Autónoma de México. Maestría en Ingeniería Petrolera y Ph. D. en Ingeniería Petrolera por la University of Tulsa.

Jubilado de Pemex. Actualmente se desempeña como profesor en la Universidad Nacional Autónoma de México.

Zhangxing (John) Chen

B.S. in Mathematics, University of Jiangxi. Master in science in Applied & Computational Mathematics, Xi'an Jiaotong University. Ph.D. in Applied & Computational Mathematics, Purdue University. Actualmente labora como professor en la University of Calgary.

María del Carmen Muñoz Ruiz

Ingeniera petrolera egresada de la ESIA Unidad Ticomán del Instituto Politécnico Nacional. Maestra en ingeniería de yacimientos, (Instituto Mexicano del Petróleo).

Actualmente se desempeña como Ingeniera de yacimientos en el Activo Litoral de Tabasco.